Analysis of the viscoelastic coefficients in the Vignale-Kohn functional

Berger, J.A.; de Boeij, P.L.; van Leeuwen, R.

Published in:
Physical Review B

DOI:
10.1103/PhysRevB.71.155104

Publication date:
2005

Analysis of the viscoelastic coefficients in the Vignale-Kohn functional: The cases of one- and three-dimensional polyacetylene

J. A. Berger, P. L. de Boeij, and R. van Leeuwen
Theoretical Chemistry, Materials Science Centre, Rijksuniversiteit Groningen, Nijenborgh 4, 9747AG Groningen, The Netherlands
(Received 23 November 2004; published 5 April 2005)

In this work we employ the Vignale-Kohn (VK) current functional in the calculation of the linear response properties of polyacetylene for both the one-dimensional infinite chain and the infinite three-dimensional crystal. We test the two existing parametrizations of the longitudinal and transverse exchange-correlation kernels of the homogeneous electron gas that enter the VK functional and show that they lead to very different results. We argue that this is mainly caused by the different values of these kernels in the zero-frequency limit in the two parametrizations. In this limit knowledge of the exchange correlation part of the shear modulus of the homogeneous electron gas becomes very important. It is exactly this quantity that is not known accurately. Furthermore, we show that our results are in good qualitative agreement with results obtained earlier using the Vignale-Kohn functional for polyacetylene oligomers.

DOI: 10.1103/PhysRevB.71.155104 PACS number(s): 71.45.Gm, 31.15.Ew, 71.10.Ca, 71.20.Rv

I. INTRODUCTION

Time-dependent density functional theory (TDDFT) developed by Runge and Gross[1] makes it possible to describe the dynamic properties of interacting many-particle systems in an exact manner.[1–4] Ghosh and Dhara[5,6] showed that the Runge-Gross theorems could be extended to systems that are subjected to general time-dependent electromagnetic fields. The method has proven to be an accurate tool in the study of electronic response properties.[3,7,8] In this work we study infinite systems for which we use time-dependent current-density functional theory (TDCDFT).[3,9–11] In this approach the electron density of TDDFT is substituted by the electron current density as the fundamental quantity. There are mainly three reasons to use TDCDFT instead of ordinary TDDFT. The first reason is related to the use of periodic boundary conditions which provide an efficient way to describe infinite systems but that artificially remove the effects of density changes at the surface.[12] For example, when a system is perturbed by an electric field there will be a macroscopic response of the system and there will be a current flowing through the interior with a nonzero average given by $\mathbf{j}(t) = (1/V)\int_V \mathbf{j}(\mathbf{r},t)\, d\mathbf{r}$, which is the spatial average of the current density $\mathbf{j}(\mathbf{r},t)$ over an arbitrary volume V. This macroscopic current is directly related through the continuity equation to a density change at the outer surface of the system but does not correspond to a density change in the bulk of the system. The density change at the surface of the system leads to a macroscopic screening field in the bulk of the system. When using periodic boundary conditions this phenomenon cannot be described with a functional of the bulk density alone[12] but it can be described by a functional of the current density in the bulk. Some of these difficulties can be circumvented by use of an expression which relates the density-density response function to the trace of the current-current response function.[8,13,14] However, for anisotropic materials this relation only provides enough information to extract the trace of the dielectric tensor and not its individual components. Second, in TDDFT only the response caused by longitudinal vector potentials can be accounted for since only purely longitudinal vector potentials can be gauge transformed to scalar potentials. The scalar potential is the natural conjugate variable of the density in the meaning of a Legendre transform.[4] However, when we consider transverse vector potentials the natural Legendre conjugate is the current density.[15] Third, to describe nonlocal exchange-correlation (xc) effects in large systems[14,16,17] it can be more convenient and more efficient to use a local functional of the current density instead of a nonlocal functional of the density.[18–20] Within TDDFT one would need an exchange-correlation functional that is completely nonlocal to be able to take into account the charges that are induced at the surface of the system caused by the external field and which produce a counteracting field.[12,21] Instead, by applying a local functional of the current density we can still take into account nonlocal effects that are induced in the system by an external field.

TDDFT has mainly been used within the adiabatic local density approximation (ALDA) in which the exchange-correlation scalar potential $v_{xc}(\mathbf{r},t)$, which is the functional derivative of the exchange-correlation energy with respect to the density, is just a local functional of the density. In this work we present another method that goes beyond the ALDA in which we employ an exchange-correlation vector potential, $\mathbf{A}_{xc}(\mathbf{r},t)$, which we approximate as a local functional of the current density using the expression derived by Vignale and Kohn.[10,11] They were the first to derive an expression for $\mathbf{A}_{xc}(\mathbf{r},t)$ that goes beyond the ALDA by formulating a local gradient expansion in terms of the current density. By studying the weakly inhomogeneous electron gas they found a dynamical exchange-correlation functional in terms of the current density that is nonlocal in time but still local in space. By applying this functional in an approximated fashion as a polarization functional we have observed that the Vignale-Kohn (VK) functional holds great promise since the dielectric functions of several semiconductors were much improved.[22] However, to obtain results in good agreement with experiment an empirical prefactor had to be used to

reduce the intensity of the spectra. Later van Faassen *et al.*[18,19] showed that the inclusion of the VK functional in TDDFT calculations provides greatly improved polarizabilities for π-conjugated polymers.

The evaluation of the VK expression for $\mathbf{A}_{xc}(\mathbf{r},t)$ requires knowledge of some properties of the homogeneous electron gas, i.e., the exchange correlation energy $e_{xc}(\rho_0)$ and the longitudinal and transverse exchange-correlation kernels, $f_{xcL}(\rho_0,\omega)$ and $f_{xcT}(\rho_0,\omega)$, respectively, where ρ_0 is the electron density of the electron gas. Knowledge of the first is already required in the ALDA and can be obtained from the accurate results of Monte Carlo calculations.[23,24] The xc kernels, on the other hand, are not known accurately. Gross and Kohn (GK) (Refs. 25 and 26) proposed an interpolation formula for $\mathrm{Im}\, f_{xcL}(\rho_0,\omega)$ in which the coefficients were obtained from sum rule arguments and exact results from second-order perturbation theory that fix the low- and high-frequency limits of this quantity. The real part can then be obtained from the Kramers-Krönig dispersion relations. Their result is exact only in the limit $\omega\to\infty$ but in the limit $\omega\to 0$ the function $\mathrm{Im}\, f_{xcL}(\rho_0,\omega)$ reduces to zero as a third power of ω instead of reducing linearly to zero. Furthermore, they do not give an expression for $\mathrm{Im}\, f_{xcT}(\rho_0,\omega)$ which renders their method inadequate for evaluation of the VK functional. Conti, Nifosì, and Tosi (CNT) (Ref. 27) chose a different route and calculated $\mathrm{Im}\, f_{xcL,T}(\rho_0,\omega)$ directly by means of an approximate decoupling of an exact four-point response function. These calculations were done under the constraint that the sum rules obtained by GK be satisfied. This means that their calculated values of $f_{xcL,T}(\rho_0,\omega)$ have the same behavior in the limit $\omega\to 0$ as the GK approximation. Their results show more structure than those of GK, in particular near twice the plasmon frequency ω_{pl}, where the contribution from two-plasmon excitations is the strongest. In addition CNT introduced a parametrization of their results which makes it applicable to the VK approach. Qian and Vignale (QV) (Ref. 28) combined the interpolation scheme of GK with the results obtained from the CNT calculations. They adopt the GK expression in which the coefficients are now chosen such as to reproduce the correct perturbative behavior in the limit $\omega\to 0$ as well as the correct behavior in the limit $\omega\to\infty$. Moreover, they have an extra parameter in their scheme which accounts for a smoothening of the two-plasmon contributions found by CNT around $\omega=2\omega_{pl}$. It is fixed by sum rules. One of the aims of this paper is to give a comparison between the CNT and QV parametrizations of $f_{xcL,T}(\rho_0,\omega)$. More specifically, we will test their influence in the application of the VK functional to the calculation of linear response properties of polyacetylene. We will show that the result strongly depends on the values of $f_{xcT}(\rho_0,\omega)$ in the limit $\omega\to 0$. In order to show this we will also evaluate the CNT and the QV parametrization in the static limit. We use polyacetylene as a test case and calculate the polarizability per unit chain length of the infinite chain (1D) and the dielectric function of crystalline polyacetylene (3D). The reason for looking at polyacetylene is to be able to connect to the work of van Faassen *et al.*[18–20] in which it was one of the π-conjugated polymers studied for which a great improvement of the polarizability was found by introducing the VK functional. We will show that in the case of the infinite polymer (1D and 3D) we obtain qualitatively similar results. The polyacetylene crystal has the so-called herring-bone structure with two polymer chains per unit cell. There exist two different configurations of polyacetylene belonging to the space groups $P2_1/a$ and $P2_1/n$. The former has an in-phase arrangement of the two chains with respect to the dimerized backbone and the latter has an antiphase arrangement. It was found that the total energy for $P2_1/a$ is slightly lower than that for $P2_1/n$ and the former can therefore be considered to be more stable.[29] In this paper we will consider polyacetylene belonging to the space group $P2_1/a$ only and therefore we will drop the specification of the space group in the remainder.

In other works, calculations have been performed to obtain the absorption spectra of 1D and 3D polyacetylene by solving the Bethe-Salpeter equation (BSE), which is an accurate and well-established method. The absorption spectrum of the 1D infinite polyacetylene chain has been calculated by Rohlfing and Louie.[30] They found two bound exciton states at excitation energies 1.7 and 1.8 eV of which only the former shows a sharp peak in the absorption spectrum; the latter has no oscillator strength for optical transitions. Puschnig and Ambrosch-Draxl[31] also performed calculations on the 1D chain as well as on the 3D crystal. Starting from a ground-state DFT calculation they obtained the absorption spectrum by solving the BSE. They rigidly shifted upwards the conduction bands found from their DFT calculation in order to obtain quasiparticle energies from the Kohn-Sham energies. In the 1D case they shifted the conduction bands such as to obtain the same energy gap as Rohlfing and Louie. Subsequently solving the BSE they find a bound exciton state with nonzero oscillator strength at excitation energy 1.55 eV. In the 3D case they find the lowest exciton state to have a binding energy of 0.05 eV but it has almost no oscillator strength for optical transitions. The main feature of the absorption spectrum they found is a broad peak at 0.5 eV above the energy gap. Recent BSE calculations by Tiago *et al.*[32] on the 3D crystal show a peak at 1.7 eV. There is also experimental data available from measurements on highly oriented polyacetylene films. The polyacetylene films are oriented by stretching. The absorption spectrum measured by Leising[33] shows a broad peak at about 1.7 eV. We have to be careful, however, when comparing to experiment since the polymer crystals often suffer from substantial static and dynamic disorder[34] and it is not clear to what extent these effects influence the results.

The outline of this article is as follows. In Sec. II we start by giving a description of the theory we use. It consists of an outline of TDCDFT and the way in which we apply it in the regime of linear response as well as an introduction to the VK functional where we discuss some of its aspects and discuss the parametrizations of the exchange-correlation kernels of the homogeneous electron gas $f_{xcL,T}(\rho_0,\omega)$ that enter the VK functional. In Sec. III we then give the main aspects of the implementation. The computational details of the calculations are the subject of Sec. IV. We have tested our method on polyacetylene (1D and 3D), the results of which can be found in Sec. V. Finally we draw conclusions from our findings in Sec. VI.

II. THEORY

A. TDCDFT

It was shown by Runge and Gross[1] that, for a given initial state, there is a one-to-one correspondence between the time-dependent density $\rho(\mathbf{r},t)$ and the time-dependent external scalar potential $v(\mathbf{r},t)$ up to a purely time-dependent function $c(t)$. Ghosh and Dhara[5,6] extended the Runge-Gross proof to systems subjected to general time-dependent electromagnetic fields by proving that, for a given initial state, there exists a one-to-one correspondence up to a gauge transformation between the time-dependent current density and the set of potentials $\mathbf{(}v(\mathbf{r},t),\mathbf{A}(\mathbf{r},t)\mathbf{)}$, in which $\mathbf{A}(\mathbf{r},t)$ is the time-dependent external vector potential (see also Ref. 3). The latter theory has the advantages that were already mentioned in the Introduction. Ghosh and Dhara further provide a practical scheme for calculating time-dependent densities and current densities. Here an interacting many-particle system in an external electromagnetic field is replaced by an auxiliary non-interacting many-particle system in an effective field. This effective field has the property that it produces the exact time-dependent current density and the exact time-dependent density for a given initial state. If the initial state is the ground state, it is already determined by the ground state density on the basis of the Hohenberg-Kohn theorem.[35] In the Kohn-Sham scheme the time-dependent single-particle wave functions are solutions of the following equation

$$i\frac{\partial}{\partial t}\psi_n(\mathbf{r},t)=\left(\frac{1}{2}\left[-i\boldsymbol{\nabla}+\frac{1}{c}\mathbf{A}_{eff}(\mathbf{r},t)\right]^2+v_{eff}(\mathbf{r},t)\right)\psi_n(\mathbf{r},t). \tag{1}$$

Atomic units (a.u.) are used throughout this work. The time-dependent effective potentials are uniquely determined (apart from an arbitrary gauge transformation) by the exact time-dependent density and current density. These exact particle densities can be obtained from the solutions of Eq. (1) for $\psi_n(\mathbf{r},t)$:

$$\rho(\mathbf{r},t)=\sum_n f_n\psi_n^*(\mathbf{r},t)\psi_n(\mathbf{r},t) \tag{2}$$

and

$$\mathbf{j}(\mathbf{r},t)=\sum_n f_n\,\mathrm{Re}[-i\psi_n^*(\mathbf{r},t)\,\boldsymbol{\nabla}\,\psi_n(\mathbf{r},t)]+\frac{1}{c}\rho(\mathbf{r},t)\mathbf{A}_{eff}(\mathbf{r},t), \tag{3}$$

where f_n are the occupation numbers of the Kohn-Sham wave functions and we assume that our initial state is described by a single Slater determinant. The first and second terms on the right-hand side of Eq. (3) correspond to the paramagnetic and diamagnetic current, respectively. The total $\mathbf{j}(\mathbf{r},t)$ is the physical gauge-invariant current density. The effective potentials of Eq. (1) consist of the externally applied potentials and potentials arising from the Hartree and xc contributions of the density and current density. We have chosen our gauge for the potentials according to Kootstra *et al.*[36,37] where for the use of periodic boundary conditions it is essential that the macroscopic part of the external field is contained in the vector potential. The scalar potential is lattice periodic and therefore cannot contain any components that represent a macroscopic field. We split the effective potentials into the following contributions:

$$\mathbf{A}_{eff}(\mathbf{r},t)=\mathbf{A}_{mac}(\mathbf{r},t)+\mathbf{A}_{xc}(\mathbf{r},t), \tag{4}$$

$$v_{eff}(\mathbf{r},t)=v_{H,mic}(\mathbf{r},t)+v_{xc,mic}(\mathbf{r},t). \tag{5}$$

Here $v_{H,mic}(\mathbf{r},t)$ is the microscopic part of the Hartree potential and $v_{xc,mic}(\mathbf{r},t)$ is the microscopic part of the exchange-correlation potential. The term $\mathbf{A}_{mac}(\mathbf{r},t)$ denotes the macroscopic vector potential,

$$\mathbf{A}_{mac}(\mathbf{r},t)=\mathbf{A}_{ext}(\mathbf{r},t)+\mathbf{A}_{ind}(\mathbf{r},t), \tag{6}$$

where $\mathbf{A}_{ext}(\mathbf{r},t)$ is the external vector potential and $\mathbf{A}_{ind}(\mathbf{r},t)$ is the induced macroscopic vector potential. The latter potential accounts for the long-range contribution of the Hartree potential of the surface charge as well as the retarded contribution of the induced transverse current density. We can safely ignore the microscopic part, because its electric field contribution is already a factor ω^2/c^2 smaller than that of the microscopic Hartree potential.[36,38,39] The gauge is chosen such that the external field is incorporated into $\mathbf{A}_{mac}(\mathbf{r},t)$. Finally, $\mathbf{A}_{xc}(\mathbf{r},t)$ is the exchange-correlation vector potential for which in practice approximations are required.

B. Linear response

To study the linear response properties of systems, which are initially in the ground state and perturbed by a time-dependent electromagnetic field, it is convenient to work in the frequency domain. To do this we use the Fourier transform which is given by

$$\mathbf{j}(\mathbf{r},t)=\int\mathbf{j}(\mathbf{r},\omega)e^{-i\omega t}\,d\omega. \tag{7}$$

Similar transforms are used for other quantities.

A time-dependent electric field $\mathbf{E}_{ext}(\omega)$ applied to a solid will induce a macroscopic polarization $\mathbf{P}_{mac}(\omega)$ which can be obtained from the induced current density by

$$\mathbf{P}_{mac}(\omega)=\frac{-i}{\omega V}\int_V\delta\mathbf{j}(\mathbf{r},\omega)\,d\mathbf{r}, \tag{8}$$

and which will be proportional to the macroscopic field $\mathbf{E}_{mac}(\omega)$, i.e., the applied field plus the average induced field within the solid. The constant of proportionality is the electric susceptibity $\chi_e(\omega)$,

$$\mathbf{P}_{mac}(\omega)=\chi_e(\omega)\cdot\mathbf{E}_{mac}(\omega). \tag{9}$$

Unlike $\mathbf{P}_{mac}(\omega)$ and $\mathbf{E}_{mac}(\omega)$, the susceptibility $\chi(\omega)$ is independent of the size and shape and is therefore a bulk property of the system. The induced current density can, in principle, be calculated from the true current-current response function $\chi_{\mathbf{jj}}(\mathbf{r},\mathbf{r}',\omega)$ of the system according to

$$\delta\mathbf{j}(\mathbf{r},\omega) = \frac{-i}{\omega}\int \chi_{\mathbf{jj}}(\mathbf{r},\mathbf{r}',\omega)\cdot\mathbf{E}_{mac}(\mathbf{r}',\omega)\,d\mathbf{r}'. \quad (10)$$

From Eqs. (8)–(10) it follows that

$$\chi_e(\omega) = \frac{-1}{\omega^2}\frac{1}{V}\int d\mathbf{r}\int d\mathbf{r}'\chi_{\mathbf{jj}}(\mathbf{r},\mathbf{r}',\omega). \quad (11)$$

The direct evaluation of the current-current response function is, however, unpractical. In our method we therefore adopt a Kohn-Sham formulation, in which the response to an external electric field of an interacting system is calculated as the response of an auxiliary noninteracting system to an effective field $(v(\mathbf{r},\omega),\mathbf{A}(\mathbf{r},\omega))$. We choose the field $\mathbf{E}_{mac}(\mathbf{r},\omega)$ to be given and its relation to $\mathbf{A}_{mac}(\mathbf{r},\omega)$ is given by $\mathbf{A}_{mac}(\mathbf{r},\omega)=c\mathbf{E}_{mac}(\mathbf{r},\omega)/i\omega$. We leave the relation between $\mathbf{E}_{mac}(\mathbf{r},\omega)$ and $\mathbf{E}_{ext}(\omega)$ unspecified as this depends on the sample size and shape and requires knowledge of $\chi_e(\omega)$. The effective vector potential of Eq. (4) has the property that it produces the exact current density in the Kohn-Sham system. From the exact current density we can calculate the exact density according to the continuity equation,

$$\boldsymbol{\nabla}\cdot\delta\mathbf{j}(\mathbf{r},\omega) = i\omega\delta\rho(\mathbf{r},\omega). \quad (12)$$

The effective field is a functional of the induced current density and it has to be solved in a self-consistent manner. To first order we have the following expressions within the Kohn-Sham scheme for the induced density,

$$\delta\rho(\mathbf{r},\omega) = \int\left(\frac{1}{c}\chi_{s,\rho\mathbf{j}}(\mathbf{r},\mathbf{r}',\omega)\cdot\delta\mathbf{A}_{eff}(\mathbf{r}',\omega) + \chi_{s,\rho\rho}(\mathbf{r},\mathbf{r}',\omega)\delta v_{eff}(\mathbf{r}',\omega)\right)d\mathbf{r}' \quad (13)$$

and the induced current density,

$$\delta\mathbf{j}(\mathbf{r},\omega) = \int\left(\frac{1}{c}[\chi_{s,\mathbf{jj}}(\mathbf{r},\mathbf{r}',\omega)+\rho_0(\mathbf{r})\delta(\mathbf{r}-\mathbf{r}')]\cdot\delta\mathbf{A}_{eff}(\mathbf{r}',\omega) + \chi_{s,\mathbf{j}\rho}(\mathbf{r},\mathbf{r}',\omega)\delta v_{eff}(\mathbf{r}',\omega)\right)d\mathbf{r}'. \quad (14)$$

Here the $\chi_{s,ab}$ are the Kohn-Sham response kernels which are properties of the ground state. They are given by

$$\chi_{s,ab}(\mathbf{r},\mathbf{r}',\omega) = \lim_{\eta\to 0}\sum_{n,n'}(f_n - f_{n'}) \times\frac{[\psi_n^*(\mathbf{r})\hat{a}\psi_{n'}(\mathbf{r})][\psi_{n'}^*(\mathbf{r}')\hat{b}\psi_n(\mathbf{r}')]}{\epsilon_n-\epsilon_{n'}+\omega+i\eta}, \quad (15)$$

in which $\hat{a}$ and $\hat{b}$ can be either $\hat{\rho}=1$ or $\hat{\mathbf{j}}=-i(\boldsymbol{\nabla}-\boldsymbol{\nabla}^\dagger)/2$. The dagger on the nabla operator indicates that the operator acts on terms to the left of it. In Eq. (15) ϵ_n are the eigenvalues of the Kohn-Sham orbitals $\psi_n(\mathbf{r})$ of the unperturbed system. The positive infinitesimal η in Eq. (15) ensures the causality of the response function.

In principle the scalar potential could have been gauge transformed into a vector potential[40,41] and $\delta\rho(\mathbf{r},\omega)$ could have been expressed in terms of $\delta\mathbf{j}(\mathbf{r},\omega)$ by means of the continuity equation, Eq. (12). For the implementation it is, however, convenient to include both the induced density and the scalar potential in our formalism.

If we neglect the small Landau diamagnetic part, which only is important in the evaluation of magnetic properties, we can use the approximate conductivity sum rule[13]

$$[\chi_{s,\mathbf{jj}}(\mathbf{r},\mathbf{r}',0)]_{ij}+\rho_0(\mathbf{r})\delta_{ij}\delta(\mathbf{r}-\mathbf{r}') = 0. \quad (16)$$

This sum rule can be used to relate the diamagnetic contribution to the induced current density $\delta\mathbf{j}_d = -\rho_0(\mathbf{r})\delta\mathbf{A}_{eff}(\mathbf{r},\omega)/c$ to the static Kohn-Sham current-current response function $\chi_{s,\mathbf{jj}}(\mathbf{r},\mathbf{r}',0)$. With this approximation we now get for the induced current density

$$\delta\mathbf{j}(\mathbf{r},\omega) = \int\left(\frac{1}{c}[\chi_{s,\mathbf{jj}}(\mathbf{r},\mathbf{r}',\omega)-\chi_{s,\mathbf{jj}}(\mathbf{r},\mathbf{r}',0)]\cdot\delta\mathbf{A}_{eff}(\mathbf{r}',\omega) + \chi_{s,\mathbf{j}\rho}(\mathbf{r},\mathbf{r}',\omega)\delta v_{eff}(\mathbf{r}',\omega)\right)d\mathbf{r}'. \quad (17)$$

This provides an efficient way to deal with the incompleteness of the basis set in the $\omega\to 0$ limit in actual applications. In Eq. (17) the effective potentials are given, to first order, by

$$\delta\mathbf{A}_{eff}(\mathbf{r},\omega) = \delta\mathbf{A}_{mac}(\mathbf{r},\omega)+\delta\mathbf{A}_{xc}(\mathbf{r},\omega), \quad (18)$$

$$\delta v_{eff}(\mathbf{r},\omega) = \delta v_{H,mic}(\mathbf{r},\omega)+\delta v_{xc,mic}(\mathbf{r},\omega). \quad (19)$$

In our gauge the use of the ALDA is equivalent to putting $\delta\mathbf{A}_{xc}(\mathbf{r},\omega)=0$, in which case the effective vector potential becomes equal to $\delta\mathbf{A}_{mac}(\mathbf{r},\omega)$. In the following we will go beyond the ALDA and give an expression for $\delta\mathbf{A}_{xc}(\mathbf{r},\omega)$ using the spin-restricted expressions of Vignale and Kohn.[10,11,42]

C. The Vignale-Kohn functional

The effective perturbing field in the Kohn-Sham Hamiltonian of Eq. (1) is in linear response given by

$$\delta\hat{h}_{eff}(\mathbf{r},t) = \delta v_{eff}(\mathbf{r},t)+\frac{1}{c}\hat{\mathbf{j}}\cdot\delta\mathbf{A}_{eff}(\mathbf{r},t), \quad (20)$$

in which the exchange-correlation contribution is given by

$$\delta\hat{h}_{xc}(\mathbf{r},t) = \delta v_{xc,mic}^{ALDA}(\mathbf{r},t)+\frac{1}{c}\hat{\mathbf{j}}\cdot\delta\mathbf{A}_{xc}(\mathbf{r},t). \quad (21)$$

This defines the gauge we use for the xc potentials, namely that all the contributions from the ALDA are contained in the scalar potential and all the contributions beyond the ALDA are contained in the vector potential. This definition is compatible with the gauge set in Eqs. (4) and (5), in which the scalar potential only contains components that represent microscopic fields. The general expression for the exchange-correlation vector potential to first order is

$$\delta\mathbf{A}_{xc}(\mathbf{r},\omega) = \int\mathbf{f}_{xc}(\mathbf{r},\mathbf{r}',\omega)\cdot\delta\mathbf{j}(\mathbf{r}',\omega)\,d\mathbf{r}', \quad (22)$$

which defines the tensor kernel $\mathbf{f}_{xc}(\mathbf{r},\mathbf{r}',\omega)$. Vignale and Kohn derived an approximation for this xc kernel.[10,11] For

this they studied a periodically modulated electron gas with wave vector **q**, i.e.,

$$\rho_0(\mathbf{r}) = \overline{\rho}(1 + 2\gamma\cos(\mathbf{q}\cdot\mathbf{r})), \tag{23}$$

where $\overline{\rho}$ is the density of the homogeneous electron gas and $\gamma \ll 1$, and performed an expansion of the xc kernel

$$\mathbf{f}_{xc}(\mathbf{k}+m\mathbf{q},\mathbf{k},\omega) = \frac{1}{V}\int d\mathbf{r}\int d\mathbf{r}'\mathbf{f}_{xc}(\mathbf{r},\mathbf{r}',\omega)e^{-i(\mathbf{k}+m\mathbf{q})\cdot\mathbf{r}}e^{i\mathbf{k}\cdot\mathbf{r}'}, \tag{24}$$

to second order in **k** and **q** and to first order in γ. In Eq. (24) V is the volume of the system and m is an integer for which to first order in γ only the values for $|m| \leqslant 1$ are needed. This expansion was shown to be analytic for small **k** and **q** and to be valid under the constraints $k, q \ll k_F, \omega/v_F$, where k_F and v_F are the Fermi momentum and the Fermi velocity, respectively. The coefficients in this expansion are completely determined in terms of the density $\overline{\rho}$ and the coefficients $f_{xcL}(\overline{\rho},\omega)$ and $f_{xcT}(\overline{\rho},\omega)$ of the xc kernel of the homogeneous electron gas by the Onsager symmetry relation, the zero-force and zero-torque theorems, and a Ward identity.[10,11] The VK expression for $\delta\mathbf{A}_{xc}(\mathbf{r},\omega)$ is then obtained from

$$\delta\mathbf{A}_{xc}(\mathbf{r},\omega) = \sum_{m=0,\pm1}\int\frac{d\mathbf{k}}{(2\pi)^3} \times\mathbf{f}_{xc}(\mathbf{k}+m\mathbf{q},\mathbf{k},\omega)e^{i(\mathbf{k}+m\mathbf{q})\cdot\mathbf{r}}\delta\mathbf{j}(\mathbf{k},\omega), \tag{25}$$

by inserting the expansion for $\mathbf{f}_{xc}$ in Eq. (25) and using Eq. (23). Since this expression contains first- and second-order powers of **k** we obtain first- and second-order derivatives of the current density in real space. Similarly, first- and second-order powers of **q** lead to first- and second-order derivatives of $\rho_0(\mathbf{r})$ in real space. The constraint $q \ll k_F, \omega/v_F$ implies in real space that

$$\frac{|\nabla\rho_0(\mathbf{r})|}{\rho_0(\mathbf{r})} \ll k_F, \omega/v_F, \tag{26}$$

where $k_F = v_F = (3\pi^2\overline{\rho})^{1/3}$. Likewise, the condition $k \ll k_F, \omega/v_F$ implies[11,43]

$$\frac{|\nabla j_i(\mathbf{r})|}{j_i(\mathbf{r})} \ll k_F, \omega/v_F. \tag{27}$$

From analysis of Eq. (25) and as a consequence of a Ward identity $\overline{\rho}$ can be replaced by $\rho_0(\mathbf{r})$ in the coefficients $f_{xcL}(\overline{\rho},\omega)$ and $f_{xcT}(\overline{\rho},\omega)$. This will only affect terms of order γ^2 which were already neglected in the derivation. By doing this we obtain a functional we can apply to general systems, although if applied to systems with large density variations we may go outside the range of validity of the VK derivation. It was shown by Vignale, Ullrich, and Conti that the VK expression for $\delta\mathbf{A}_{xc}(\mathbf{r},\omega)$ could be written in the form of a viscoelastic field[42,44]

$$\frac{i\omega}{c}\delta\mathbf{A}_{xc,i}(\mathbf{r},\omega) = -\frac{1}{\rho_0(\mathbf{r})}\sum_j\partial_j\sigma_{xc,ij}(\mathbf{r},\omega), \tag{28}$$

where $\sigma_{xc}(\mathbf{r},\omega)$ is a tensor field which has the structure of a symmetric viscoelastic stress tensor,

$$\sigma_{xc,ij} = \tilde{\eta}_{xc}\left(\partial_j u_i + \partial_i u_j - \frac{2}{3}\delta_{ij}\sum_k\partial_k u_k\right) + \tilde{\zeta}\delta_{ij}\sum_k\partial_k u_k \tag{29}$$

in which the velocity field $\mathbf{u}(\mathbf{r},\omega)$ is given by

$$\mathbf{u}(\mathbf{r},\omega) = \frac{\delta\mathbf{j}(\mathbf{r},\omega)}{\rho_0(\mathbf{r})}. \tag{30}$$

The coefficients $\tilde{\eta}_{xc}(\mathbf{r},\omega)$ and $\tilde{\zeta}_{xc}(\mathbf{r},\omega)$ are determined by the transverse and longitudinal response coefficients $f_{xcT}(\rho_0(\mathbf{r}),\omega)$ and $f_{xcL}(\rho_0(\mathbf{r}),\omega)$ of the homogeneous electron gas evaluated at the density $\rho_0(\mathbf{r})$,

$$\tilde{\eta}_{xc}(\mathbf{r},\omega) = \frac{i}{\omega}\rho_0^2(\mathbf{r})f_{xcT}(\rho_0(\mathbf{r}),\omega), \tag{31}$$

and

$$\tilde{\zeta}_{xc}(\mathbf{r},\omega) = \frac{i}{\omega}\rho_0^2(\mathbf{r})\left(f_{xcL}(\rho_0(\mathbf{r}),\omega) - \frac{4}{3}f_{xcT}(\rho_0(\mathbf{r}),\omega) - \frac{d^2e_{xc}}{d\rho^2}(\rho_0(\mathbf{r}))\right), \tag{32}$$

where $e_{xc}(\rho_0(\mathbf{r}))$ is the exchange-correlation energy per unit volume of the homogeneous electron gas. The quantities $\tilde{\eta}_{xc}(\mathbf{r},\omega)$ and $\tilde{\zeta}_{xc}(\mathbf{r},\omega)$ can be interpreted as viscoelastic coefficients.[42,44] The parameter $\tilde{\zeta}_{xc}(\mathbf{r},\omega)$ contains a factor for which one can prove the exact relation[42,44]

$$\lim_{\omega\to0}\left(f_{xcL}(\rho_0,\omega) - \frac{4}{3}f_{xcT}(\rho_0,\omega) - \frac{d^2e_{xc}}{d\rho^2}(\rho_0)\right) = 0. \tag{33}$$

From Eq. (28) we can now derive an expression for the exchange-correlation kernel in real space for which we obtain

$$f_{xc,ij}(\mathbf{r},\mathbf{r}',\omega) = \frac{c}{i\omega}\frac{1}{\rho_0(\mathbf{r})\rho_0(\mathbf{r}')}\left(\partial_j\partial_i' + \delta_{ij}\sum_k\partial_k\partial_k' - \frac{2}{3}\partial_i\partial_j'\right) \times[\delta(\mathbf{r}-\mathbf{r}')\tilde{\eta}_{xc}(\mathbf{r},\omega)] + \frac{c}{i\omega}\frac{1}{\rho_0(\mathbf{r})\rho_0(\mathbf{r}')}\partial_i\partial_j'[\delta(\mathbf{r}-\mathbf{r}')\tilde{\zeta}_{xc}(\mathbf{r},\omega)]. \tag{34}$$

Note that $f_{xc,ij}$ satisfies the Onsager symmetry relation,[11] i.e.,

$$f_{xc,ij}(\mathbf{r},\mathbf{r}',\omega) = f_{xc,ji}(\mathbf{r}',\mathbf{r},\omega), \tag{35}$$

and it is clear from Eq. (34) that $\mathbf{f}_{xc}$ is local in space but nonlocal in time.

D. The response coefficients

The longitudinal and transverse response kernels $f_{xcL}(\rho_0,\omega)$ and $f_{xcT}(\rho_0,\omega)$ still have to be specified. These

functions are well studied for the electron gas.[27,28,44–46] In **q**-space they are defined as

$$\lim_{q\to 0} f_{xcL(T)}(\mathbf{q},\omega) \equiv f_{xcL(T)}(\omega) = \lim_{q\to 0}\frac{\omega^2}{q^2} \times (\chi^{-1}_{0,L(T)}(\mathbf{q},\omega) - \chi^{-1}_{L(T)}(\mathbf{q},\omega)) - v_{L(T)}(\mathbf{q}), \tag{36}$$

where $\chi_{L(T)}(\mathbf{q},\omega)$ is the current-current longitudinal (transverse) response function of the homogeneous electron gas, $\chi_{0,L(T)}(\mathbf{q},\omega)$ are the equivalent response functions of the noninteracting homogeneous electron gas, $v_L(\mathbf{q})=4\pi/q^2$ is the Fourier transform of the Coulomb potential, and $v_T(\mathbf{q})=0$. The identity $\lim_{\mathbf{q}\to 0} f_{xcL(T)}(q,\omega)\equiv f_{xcL(T)}(\omega)$ was obtained by Vignale and Kohn.[11,41] Note that $f_{xcL}(\mathbf{q},\omega)$ as defined in Eq. (36) coincides with $f_{xc}(\mathbf{q},\omega)$ from scalar TDDFT and it can thus be related to the local field correction $G(\mathbf{q},\omega)$ according to

$$f_{xcL}(\mathbf{q},\omega) = -v_L(\mathbf{q})G(\mathbf{q},\omega). \tag{37}$$

Since $f_{xcL,T}(\mathbf{q},\omega)$ are analytic functions of ω in the upper half of the complex ω-plane and approach real functions $f_{xcL,T}(q,\infty)$ for $\omega\to\infty$ they satisfy the standard Kramers-Krönig relations,

$$\mathrm{Re}\, f_{xcL,T}(\mathbf{q},\omega) = f_{xcL,T}(\mathbf{q},\infty) + P\int_{-\infty}^{\infty}\frac{d\omega'}{\pi}\frac{\mathrm{Im}\, f_{xcL,T}(\mathbf{q},\omega')}{\omega'-\omega}, \tag{38}$$

$$\mathrm{Im}\, f_{xcL,T}(\mathbf{q},\omega) = -P\int_{-\infty}^{\infty}\frac{d\omega'}{\pi}\frac{\mathrm{Re}\, f_{xcL,T}(\mathbf{q},\omega') - f_{xcL,T}(\mathbf{q},\infty)}{\omega'-\omega}, \tag{39}$$

where P denotes the principle value of the integral. The response functions $\chi_{0,L,T}(\mathbf{q},\omega)$ in Eq. (36) are well-known functions first calculated by Lindhard[47] and are given by

$$\chi_{0,L}(\mathbf{q},\omega) = \lim_{\eta\to 0}\frac{\omega^2}{q^2}\int\frac{d\mathbf{k}}{(2\pi)^3}\frac{f(\epsilon_{\mathbf{k}}) - f(\epsilon_{\mathbf{k}+\mathbf{q}})}{\omega - (\epsilon_{\mathbf{k}+\mathbf{q}} - \epsilon_{\mathbf{k}}) + i\eta} \tag{40}$$

and

$$\chi_{0,T}(\mathbf{q},\omega) = \rho_0 + \lim_{\eta\to 0}\frac{1}{2}\int\frac{d\mathbf{k}}{(2\pi)^3} \times\left(k^2 - \frac{(\mathbf{k}\cdot\mathbf{q})^2}{q^2}\right)\frac{f(\epsilon_{\mathbf{k}}) - f(\epsilon_{\mathbf{k}}+\mathbf{q})}{\omega - (\epsilon_{\mathbf{k}+\mathbf{q}} - \epsilon_{\mathbf{k}}) + i\eta}, \tag{41}$$

where $\epsilon_k = k^2/2$ is the free particle energy and $f(\epsilon_{\mathbf{k}})$ is the Fermi distribution function. The full response functions $\chi_{L,T}(\mathbf{q},\omega)$ are not known analytically though. There are, however, well-known exact features of $\chi_{L,T}(\mathbf{q},\omega)$ and $G(\mathbf{q},\omega)$ in the limit $q\to 0$ obtained from sum rules and results from second-order perturbative expansions. From these features and the relations (36) and (37) Gross and Kohn (GK) obtained exact properties of $f_{xcL}(\mathbf{q}=0,\omega)\equiv f_{xcL}(\omega)$ in the low- and high-frequency limits.[25,26] Furthermore, they introduced an interpolation formula for $\mathrm{Im}\, f_{xcL}(\omega)$ which reduces to the exact high-frequency limit for $\omega\to\infty$ obtained from second-order perturbative expansions by Glick and Long[48,49] and vanishes linearly in the limit $\omega\to 0$. The low-frequency behavior was determined from the $\omega\to 0$ limit of the $q\to 0$ limit of Eq. (38) resulting in the following sum rule,

$$f_{xcL}(0) - f_{xcL}(\infty) = P\int_{-\infty}^{\infty}\frac{d\omega}{\pi}\frac{\mathrm{Im}\, f_{xcL}(\omega)}{\omega}, \tag{42}$$

where $f_{xcL}(0)$ was obtained from the compressibility sum rule[50]

$$\lim_{q\to 0}\lim_{\omega\to 0} f_{xcL}(q,\omega) = \frac{K_{xc}}{\rho_0^2}, \tag{43}$$

where K_{xc} is the exchange-correlation part of the bulk modulus given by

$$K_{xc} = \rho_0^2\frac{d^2 e_{xc}(\rho_0)}{d\rho^2}, \tag{44}$$

and $f_{xcL}(\infty)$ was obtained from the third-frequency-moment sum rule.[26,50] However, the compressibility sum rule contains $\lim_{q\to 0}\lim_{\omega\to 0} f_{xcL}(q,\omega)$, which is not the same as $\lim_{\omega\to 0}\lim_{q\to 0} f_{xcL}(q,\omega)$ entering Eq. (42) as was tacitly assumed by GK. This difference was first pointed out by Conti and Vignale[44] and will be briefly discussed below. The real part of $\mathrm{Im}\, f_{xcL}(\omega)$ can subsequently be obtained from Eq. (38) evaluated at $q=0$.

A different approach to obtain $f_{xcL}(\omega)$ as well as $f_{xcT}(\omega)$ was given by Conti, Nifosì, and Tosi (CNT).[27] They calculated $\mathrm{Im}\, f_{xcL,T}(\omega)$ by direct evaluation of the imaginary parts of the current-current response functions, $\mathrm{Im}\, \chi_{L,T}(\mathbf{q},\omega)$. CNT used an exact expression for $\mathrm{Im}\, \chi_{L,T}(\mathbf{q},\omega)$ in terms of four-point response functions which were subsequently approximated by decoupling them into products of two-point response functions. In order to include the effect of plasmons the two-point response functions were then taken to be the RPA response functions. This decoupling scheme only keeps direct contributions and neglects exchange processes. To account for the latter processes CNT introduced a phenomenological factor which reduces the total two-pair spectral weight by a factor of 2 in the high-frequency limit in order to coincide with the results from second-order perturbative expansions mentioned above. In the low-frequency limit the factor is close to unity at metallic densities, thereby largely neglecting exchange processes. A distinct feature of the CNT result is a pronounced peak at $\omega=2\omega_{pl}$ in $\mathrm{Im}\, f_{xcL,T}(\omega)$, where ω_{pl} is the plasmon frequency. Since the double excitations take up most of the spectral strength and the plasmon excitation is large with respect to single-pair excitations, the spectral strength accumulates around $\omega=2\omega_{pl}$. Furthermore, CNT introduced parametrizations for $\mathrm{Im}\, f_{xcL,T}(\omega)$ that reproduce their numerical results. The real parts can again be obtained from the Kramers-Krönig relation (38) where the high-frequency limits of $f_{xcL,T}(\omega)$ are given by CNT, the expression for the longitudinal kernel being in agreement with the results of Glick and Long.[48] It must be noted that, like GK, CNT obtained the low-frequency limit of $f_{xcL}(\omega)$ by

invoking the compressibility sum rule, thereby interchanging the order of the limits. They expect the discontinuity in the limit $(q,\omega)\to(0,0)$ to be small, however, and they therefore prefer to enforce equality of the order of limits.[27] It is then interesting that, within the accuracy of their model, they found $f_{xcT}(\omega=0)$ to be indistinguishable from zero in their calculations.

Conti and Vignale[44] later obtained exact expressions for $\lim_{\omega\to0}\lim_{q\to0} f_{xcL,T}(q,\omega)$ by comparing the microscopic linear-response equations with the macroscopic viscoelastic equation of motion. Their evaluations led to the following identities for the three-dimensional electron gas,

$$\lim_{\omega\to0}\lim_{q\to0} f_{xcL}(\mathbf{q},\omega) \equiv f_{xcL}(0) = \frac{1}{\rho_0^2}\left(K_{xc}+\frac{4}{3}\mu_{xc}\right), \quad (45)$$

$$\lim_{\omega\to0}\lim_{q\to0} f_{xcT}(\mathbf{q},\omega) \equiv f_{xcT}(0) = \frac{\mu_{xc}}{\rho_0^2}, \quad (46)$$

where μ_{xc} is the exchange-correlation part of the shear modulus. [From the above identities together with Eq. (44) follows immediately Eq. (33).] The shear modulus remains finite in the $\omega\to0$ limit because the $q\to0$ limit is taken before the $\omega\to0$ limit. Taking the reverse order of limits would result in a shear modulus equal to zero. In that limit, however, $f_{xcT}(\mathbf{q},\omega)$ is no longer related to the shear modulus, but to the diamagnetic susceptibility, which is very small. Conti and Vignale further show that μ_{xc} can be related to the Landau parameters F_l according to

$$\mu_{xc} = \frac{2\rho_0 E_F}{5}\frac{F_2/5 - F_1/3}{1+F_1/3}. \quad (47)$$

Comparing Eqs. (43) and (45) it becomes immediately clear that interchanging the order of the limits for $\lim_{\omega\to0}\lim_{q\to0} f_{xcL,T}(q,\omega)$ is equivalent to the approximation $\mu_{xc}=0$, and from Eq. (46) we see that this means $f_{xcT}(0)=0$ as observed by CNT. In a subsequent paper, Nifosì, Conti, and Tosi (NCT) (Ref. 46) drop the restriction on $f_{xcL}(0)$ imposed by the compressibility sum rule and their calculations then show a nonvanishing $f_{xcT}(0)$. However, they do not expect their values for $f_{xcT}(0)$ to be very accurate as they are obtained from the integration over the whole frequency range of $\mathrm{Im}\, f_{xcT}(\omega)$ in Eq. (38).

Qian and Vignale (QV) (Ref. 28) combined the methods of GK and CNT. They obtained an analytic result for the slope of $\mathrm{Im}\, f_{xcT}(\omega)$ at $\omega=0$ by evaluating $\mathrm{Im}\,\chi_{L,T}(\mathbf{q},\omega)$ within perturbation theory in a similar way as CNT. The direct contributions were treated the same, but QV also included their exchange counterparts in the evaluation. They adopted the interpolation scheme of GK for $\mathrm{Im}\, f_{xcT}(\omega)$ but with the coefficients now determined by their analytic result for the slope at $\omega=0$ and the correct low-frequency limits, Eqs. (45) and (46), as well as the correct high-frequency behavior. The values for μ_{xc} were obtained from the Landau parameters calculated for some values of r_s in Ref. 51. To model the two-plasmon contribution identified by CNT they include an extra parameter in their interpolation scheme, i.e., the width of a Gaussian peak centered at $\omega=2\omega_{pl}$. Their model shows a peak that is less pronounced than CNT's.

From Eqs. (31)–(33) we can now determine the behavior of $\tilde{\eta}_{xc}(\mathbf{r},\omega)$ and $\tilde{\zeta}_{xc}(\mathbf{r},\omega)$ in the limit $\omega\to0$. We obtain

$$\lim_{\omega\to0}\omega\tilde{\eta}_{xc}(\mathbf{r},\omega) = i\rho_0^2(\mathbf{r}) f_{xcT}(\rho_0,0) \quad (48)$$

and

$$\lim_{\omega\to0}\omega\tilde{\zeta}_{xc}(\mathbf{r},\omega) = 0. \quad (49)$$

So only the imaginary part of $\omega\tilde{\eta}_{xc}(\mathbf{r},\omega)$ remains finite in this limit and $\omega\tilde{\zeta}_{xc}(\mathbf{r},\omega)$ vanishes identically. In this limit the CNT parametrization obviously reduces to the ALDA, as it was constructed under the assumption $f_{xcT}(\rho_0,0)=0$. However, the VK functional can be evaluated in the static limit with the NCT and QV values for $f_{xcT}(\rho_0,0)$.

To summarize, the various parametrizations of $f_{xcL,T}(\rho_0,\omega)$ presented above are denoted by CNT and QV for the completely frequency-dependent parametrizations, given in Refs. 27 and 28, respectively, whereas NCT and QV0 are frequency-independent parametrizations. NCT takes its values for $f_{xcT}(\rho_0(\mathbf{r}),0)$ from Ref. 46 and QV0 is simply the static limit of the QV parametrization. Note that the static limit of the CNT parametrization is the ALDA. These four parametrizations will be used in our calculations.

III. IMPLEMENTATION

We will show that we can write $\delta\mathbf{A}_{xc}(\mathbf{r},\omega)$ as expressed in Eqs. (28)–(30) in a more convenient way,

$$\delta\mathbf{A}_{xc}(\mathbf{r},\omega) = -\frac{ic}{\omega}\boldsymbol{\nabla}\,\delta u_{xc}(\mathbf{r},\omega) + \delta\mathbf{a}_{xc}(\mathbf{r},\omega) + \boldsymbol{\nabla}\times\delta\mathbf{b}_{xc}(\mathbf{r},\omega). \quad (50)$$

Here $\delta u_{xc}(\mathbf{r},\omega)$ is a scalar field, $\delta\mathbf{a}_{xc}(\mathbf{r},\omega)$ is a polar vector field, and $\delta\mathbf{b}_{xc}(\mathbf{r},\omega)$ is an axial vector field. There is much freedom in choosing the contributions $\delta u_{xc}(\mathbf{r},\omega)$, $\delta\mathbf{a}_{xc}(\mathbf{r},\omega)$, and $\delta\mathbf{b}_{xc}(\mathbf{r},\omega)$, and we choose a form that involves only the local values of $\delta\mathbf{j}(\mathbf{r},\omega)$, $\boldsymbol{\nabla}\cdot\delta\mathbf{j}(\mathbf{r},\omega)=i\omega\delta\rho(\mathbf{r},\omega)$, and $\boldsymbol{\nabla}\times\delta\mathbf{j}(\mathbf{r},\omega)=\delta\mathbf{m}(\mathbf{r},\omega)$ (for a detailed derivation see the Appendix):

$$\delta u_{xc} = -i\omega\frac{\frac{4}{3}\tilde{\eta}_{xc}+\tilde{\zeta}_{xc}}{\rho_0^2}\delta\rho + \left(\frac{\frac{4}{3}\tilde{\eta}_{xc}+\tilde{\zeta}_{xc}}{\rho_0^2}\frac{\boldsymbol{\nabla}\rho_0}{\rho_0} - 2\frac{\boldsymbol{\nabla}\tilde{\eta}_{xc}}{\rho_0^2}\right)\cdot\delta\mathbf{j}, \quad (51)$$

$$\frac{i\omega}{c}\delta\mathbf{a}_{xc} = -i\omega\left(\frac{\frac{4}{3}\tilde{\eta}_{xc}+\tilde{\zeta}_{xc}}{\rho_0^2}\frac{\nabla\rho_0}{\rho_0} - 2\frac{\nabla\tilde{\eta}_{xc}}{\rho_0^2}\right)\delta\rho + \frac{\tilde{\eta}_{xc}}{\rho_0^2}\frac{\nabla\rho_0}{\rho_0} \times \delta\mathbf{m} + \left(\frac{\frac{1}{3}\tilde{\eta}_{xc}+\tilde{\zeta}_{xc}}{\rho_0^2}\frac{\nabla\rho_0\otimes\nabla\rho_0}{\rho_0^2} - 2\frac{\nabla\tilde{\eta}_{xc}\otimes\nabla\rho_0+\nabla\rho_0\otimes\nabla\tilde{\eta}_{xc}}{\rho_0^3}\right)\cdot\delta\mathbf{j} + \left(2\frac{\nabla\otimes\nabla\tilde{\eta}_{xc}}{\rho_0^2} + \frac{\tilde{\eta}_{xc}}{\rho_0^2}\frac{|\nabla\rho_0|^2}{\rho_0^2}\mathbf{I}\right)\cdot\delta\mathbf{j}, \tag{52}$$

$$\frac{i\omega}{c}\delta\mathbf{b}_{xc} = \frac{\tilde{\eta}_{xc}}{\rho_0^2}\delta\mathbf{m} - \frac{\tilde{\eta}_{xc}}{\rho_0^2}\frac{\nabla\rho_0}{\rho_0}\times\delta\mathbf{j}. \tag{53}$$

The functions $\delta\rho(\mathbf{r},\omega)$, $\delta\mathbf{j}(\mathbf{r},\omega)$, and $\delta\mathbf{m}(\mathbf{r},\omega)$ can all be obtained by using at most first-order derivatives of the orbitals.

We are now able to write Eqs. (51)–(53) in the following compact and elegant matrix vector product:

$$\begin{pmatrix}\delta u_{xc}\\ i\omega\delta\mathbf{a}_{xc}/c\\ i\omega\delta\mathbf{b}_{xc}/c\end{pmatrix} = \begin{pmatrix}y_{\rho\rho} & y_{\rho\mathbf{j}} & 0\\ y_{\mathbf{j}\rho} & y_{\mathbf{jj}} & y_{\mathbf{jm}}\\ 0 & y_{\mathbf{mj}} & y_{\mathbf{mm}}\end{pmatrix}\begin{pmatrix}\delta\rho\\ i\delta\mathbf{j}/\omega\\ i\delta\mathbf{m}/\omega\end{pmatrix}. \tag{54}$$

The matrix entries are given as

$$y_{\rho\rho} = -i\omega\frac{\frac{4}{3}\tilde{\eta}_{xc}+\tilde{\zeta}_{xc}}{\rho_0^2}, \tag{55}$$

$$y_{\rho\mathbf{j}} = y_{\mathbf{j}\rho}^T = -i\omega\left(\frac{\frac{4}{3}\tilde{\eta}_{xc}+\tilde{\zeta}_{xc}}{\rho_0^2} - 2\frac{\tilde{\eta}'_{xc}}{\rho_0}\right)\frac{\nabla\rho_0}{\rho_0}, \tag{56}$$

$$y_{\mathbf{jj}} = -i\omega\left(\frac{\frac{1}{3}\tilde{\eta}_{xc}+\tilde{\zeta}_{xc}}{\rho_0^2} - 4\frac{\tilde{\eta}'_{xc}}{\rho_0} + 2\tilde{\eta}''_{xc}\right)\frac{\nabla\rho_0\otimes\nabla\rho_0}{\rho_0^2} - i\omega\left(2\frac{\tilde{\eta}'_{xc}}{\rho_0}\frac{\nabla\otimes\nabla\rho_0}{\rho_0} + \frac{\tilde{\eta}_{xc}}{\rho_0^2}\frac{|\nabla\rho_0|^2}{\rho_0^2}\mathbf{I}\right), \tag{57}$$

$$y_{\mathbf{jm}} = y_{\mathbf{mj}}^T = -i\omega\frac{\tilde{\eta}_{xc}}{\rho_0^2}\left[\frac{\nabla\rho_0}{\rho_0}\times\right], \tag{58}$$

$$y_{\mathbf{mm}} = -i\omega\frac{\tilde{\eta}_{xc}}{\rho_0^2}\mathbf{I}, \tag{59}$$

in which we define the antisymmetric 3×3 matrix $[\nabla\rho_0/\rho_0\times]_{ij} = -\Sigma_k\epsilon_{ijk}(\partial_k\rho_0)/\rho_0$ and where $\tilde{\eta}'_{xc}(\mathbf{r},\omega)$ and $\tilde{\eta}''_{xc}(\mathbf{r},\omega)$ are the first- and second-order derivatives of $\tilde{\eta}_{xc}(\mathbf{r},\omega)$ with respect to the ground-state density. The matrix in Eq. (54) is a local function of the ground state density and its first- and second-order gradients and has additional ω dependence through the coefficients $\tilde{\eta}_{xc}(\mathbf{r},\omega)$ and $\tilde{\zeta}_{xc}(\mathbf{r},\omega)$.

The xc contribution to the perturbation as written in Eq. (21) can now be written as

$$\delta\hat{h}_{xc}(\mathbf{r},t) = \delta v_{xc}^{ALDA}(\mathbf{r},t) + \delta u_{xc}(\mathbf{r},t) + \frac{1}{c}\hat{\mathbf{j}}\cdot\delta\mathbf{a}_{xc}(\mathbf{r},t) + \frac{1}{c}\hat{\mathbf{m}}\cdot\delta\mathbf{b}_{xc}(\mathbf{r},t), \tag{60}$$

in which $\hat{\mathbf{m}} = -i(\nabla^\dagger\times\nabla)$. An expression for $\delta\mathbf{m}(\mathbf{r},\omega)$ is obtained from Eq. (14) by taking the curl on either side which amounts to the substitution of $\hat{\mathbf{m}}$ for $\hat{a}$ in Eq. (15).

Using Eq. (60) the self-consistent linear-response equations can be written in the following form

$$\begin{pmatrix}\delta\rho\\ i\delta\mathbf{j}/\omega\\ i\delta\mathbf{m}/\omega\end{pmatrix} = \begin{pmatrix}\chi_{s,\rho\rho} & -i\chi_{s,\rho\mathbf{j}}/\omega & -i\chi_{s,\rho\mathbf{m}}/\omega\\ i\chi_{s,\mathbf{j}\rho}/\omega & \Delta\chi_{s,\mathbf{jj}}/\omega^2 & \Delta\chi_{s,\mathbf{jm}}/\omega^2\\ i\chi_{s,\mathbf{m}\rho}/\omega & \Delta\chi_{s,\mathbf{mj}}/\omega^2 & \Delta\chi_{s,\mathbf{mm}}/\omega^2\end{pmatrix} \times\begin{pmatrix}\delta v_{H,mic}+\delta v_{xc,mic}^{ALDA}+\delta u_{xc}\\ i\omega(\delta\mathbf{A}_{mac}+\delta\mathbf{a}_{xc})/c\\ i\omega\delta\mathbf{b}_{xc}/c\end{pmatrix}. \tag{61}$$

This relation has been written in such a way that all matrix elements are real and finite for nonmetals in the limit $\omega\to0$ as follows from the following explicit expressions for the various response kernels:

$$\chi_{s,\rho\rho}(\mathbf{r},\mathbf{r}',\omega) = \sum_{n,n'} w_{nn'}(\omega)(\psi_n^*(\mathbf{r})\psi_{n'}(\mathbf{r})\psi_{n'}^*(\mathbf{r}')\psi_n(\mathbf{r}')) \tag{62}$$

$$-\frac{i}{\omega}\chi_{s,\rho\mathbf{a}}(\mathbf{r},\mathbf{r}',\omega) = \sum_{n,n'} w_{nn'}(\omega) \times\left(\psi_n^*(\mathbf{r})\psi_{n'}(\mathbf{r})\frac{i\psi_{n'}^*(\mathbf{r}')\hat{\mathbf{a}}\psi_n(\mathbf{r}')}{\epsilon_n-\epsilon_{n'}}\right) \tag{63}$$

$$\frac{i}{\omega}\chi_{s,\mathbf{a}\rho}(\mathbf{r},\mathbf{r}',\omega) = \sum_{n,n'} w_{nn'}(\omega) \times\left(\frac{i\psi_n^*(\mathbf{r}')\hat{\mathbf{a}}\psi_{n'}(\mathbf{r}')}{\epsilon_{n'}-\epsilon_n}(\mathbf{r}')\psi_{n'}^*(\mathbf{r})\psi_n(\mathbf{r})\right) \tag{64}$$

$$\frac{1}{\omega^2}\Delta\chi_{s,\mathbf{ab}}(\mathbf{r},\mathbf{r}',\omega) = \frac{1}{\omega^2}[\chi_{s,\mathbf{ab}}(\omega)-\chi_{s,\mathbf{ab}}(\omega=0)] = \sum_{n,n'} w_{nn'}(\omega) \times\left(\frac{i\psi_n^*(\mathbf{r})\hat{\mathbf{a}}\psi_{n'}(\mathbf{r})}{\epsilon_{n'}-\epsilon_n}\frac{i\psi_{n'}^*(\mathbf{r}')\hat{\mathbf{b}}\psi_n(\mathbf{r}')}{\epsilon_n-\epsilon_{n'}}\right), \tag{65}$$

where $\hat{\mathbf{a}}$ and $\hat{\mathbf{b}}$ can be either $\hat{\mathbf{j}}$ or $\hat{\mathbf{m}}$. We have defined

$$w_{nn'}(\omega) = \frac{(f_n - f_{n'})(\epsilon_n - \epsilon_{n'})}{(\epsilon_n - \epsilon_{n'})^2 - (\omega + i\eta)^2} \tag{66}$$

as the frequency-dependent transition weights. In the periodic systems we study here n is a multi-index composed of the band index and the Bloch vector. The transition weights are included in the now ω-dependent quadrature scheme of the Brillouin zone in order to handle the singular denominator analytically as in Kootstra *et al.*[36,37]

IV. COMPUTATIONAL DETAILS

The implementation was done in the ADF-BAND program[36,52–54] and we performed our calculations with this modified version. We made use of Slater-type orbitals (STO) in combination with frozen cores and a hybrid valence basis set consisting of the numerical solutions of a free-atom Herman-Skillman program[55] that solves the radial Kohn-Sham equations. The spatial resolution of this basis is equivalent to a STO triple-zeta basis set augmented with two polarization functions. This valence basis set was made orthogonal to the core states. The Herman-Skillman program also provides us with the free-atom effective potential. The Hartree potential was evaluated using an auxiliary basis set of STO functions to fit the deformation density in the ground-state calculation and the induced density in the response calculation. We used the VK xc kernel of Eq. (34) to calculate the polarizability per unit chain length of an infinite polyacetylene chain and the macroscopic dielectric function of an infinite polyacetylene crystal. They are both semiconducting materials. In the 1D case we use the geometry given in Fig. 1 of Ref. 18. For the crystal we use the experimental structural parameters given in Table II of Ref. 29 with the exception that we put β equal to 90 deg. We used Eqs. (8) and (9) to obtain $\chi_e(\omega)$ from which the macroscopic dielectric function can directly be obtained through $\epsilon(\omega)=1+4\pi\chi_e(\omega)$. To obtain the polarizability per unit chain length of the 1D polyacetylene chain we used $\mathbf{E}_{mac}(\omega)=\mathbf{E}_{ext}(\omega)$ which is justified in the 1D case for a nonconducting system. This will be the subject of a separate paper. For the evaluation of the **k**-space integrals we used a numerical integration scheme with 23 (1D) and 110 (3D) symmetry-unique sample points in the irreducible wedge of the Brillouin zone which was constructed by adopting a Lehmann-Taut tetrahedron scheme.[56] Since in the 3D calculation the dispersion in the direction of the chain is larger than perpendicular to the chain, the sampling in the direction of the chain was 11 times denser than in the direction perpendicular to it, thereby limiting the total number of **k** points. We checked the convergence with respect to the number of conduction bands used and found that ten conduction bands are sufficient. This number was used in all our calculations. We made use of the Vosko-Wilk-Nusair parametrization[24] of the LDA exchange-correlation potential which was also used to construct the ALDA exchange-correlation kernel. As mentioned above the values of $f_{xcL,T}(\rho_0,\omega)$ were obtained from the parametrizations given in Refs. 27 and 28 denoted by CNT and QV, respectively, and the values of $f_{xcL,T}(\rho_0,0)$ were taken from Refs. 28 and 46 denoted by QV0 and NCT, respectively. However, $f_{xcL,T}(\rho_0,\omega)$ are known only at specific values of the Wigner-Seitz radius r_s ($4\pi r_s^3/3=1/\rho_0$). We used a cubic spline interpolation to obtain values of $f_{xcL,T}(\rho_0,\omega)$ at arbitrary r_s in which the behavior for small r_s was taken to be quadratic similar to exchange-only behavior. A plot of $f_{xcT}(\rho_0,0)$ from NCT and QV0 can be found in Fig. 1.

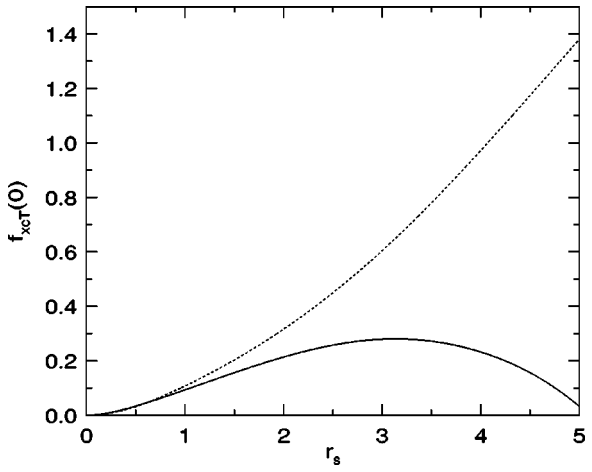

FIG. 1. $f_{xcT}(\rho_0,0)$ in a.u. for values of r_s up to $r_s=5$. Continuous curve: NCT; dashed curve: QV0. The meanings of the abbreviations are explained in the text.

V. RESULTS

In Figs. 2 and 3 we show the effect of the VK xc kernel $\mathbf{f}_{xc}(\mathbf{r},\mathbf{r}',\omega)$ given in Eq. (34) on the polarizability per unit chain length of 1D polyacetylene and on the macroscopic dielectric function of 3D polyacetylene, respectively. The various results correspond to different approximations of $f_{xcL,T}(\rho_0,\omega)$ that enter $\mathbf{f}_{xc}(\mathbf{r},\mathbf{r}',\omega)$. We compare our results obtained with the VK functional with our ALDA results, in which the xc vector potential is neglected. It clearly shows in Figs. 2 and 3 that the CNT and QV parametrizations of $f_{xcL,T}(\rho_0(\mathbf{r}),\omega)$ give drastically different results. Whereas the CNT spectra are relatively close to the ALDA spectra, the QV spectra differ strongly from them. Let us first take a look at the absorption spectrum in the 1D case. We see that the CNT spectrum has roughly the same structure as the ALDA spectrum with the exception that it shows absorption at energies below the Kohn-Sham gap. This is caused by the fact that we now consider complex values of $f_{xcL,T}(\rho_0,\omega)$. The main peak in the QV spectrum on the other hand is shifted by about 2.5 eV to higher frequency with respect to the ALDA spectrum and shows a much smoother structure. An accompanying effect of the shift is that the absorption intensity of the peak in the QV spectrum is much smaller than in the ALDA spectrum because the absorption intensity scales inversely with the square of the frequency at which the absorption occurs. Other effects may also have contributed to this lowering of intensity. Close to the QV spectrum lies the QV0 spectrum which shows that approximating the QV parametri-

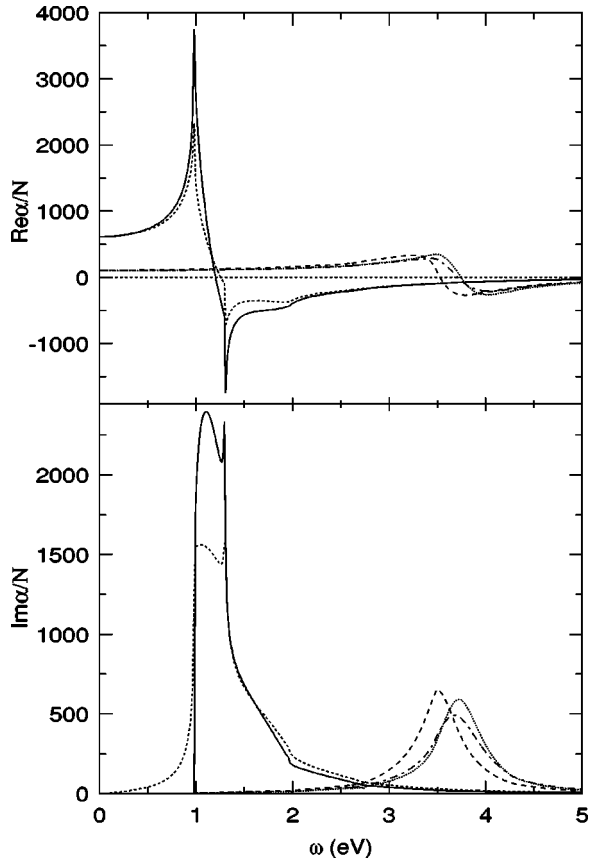

FIG. 2. The real and imaginary parts of the polarizability per unit length of an infinite polyacetylene chain in a.u. Dashed curve: CNT; long-dashed curve: NCT; dot-dashed curve: QV; dotted curve: QV0; continuous curve: ALDA. The meanings of the abbreviations are explained in the text.

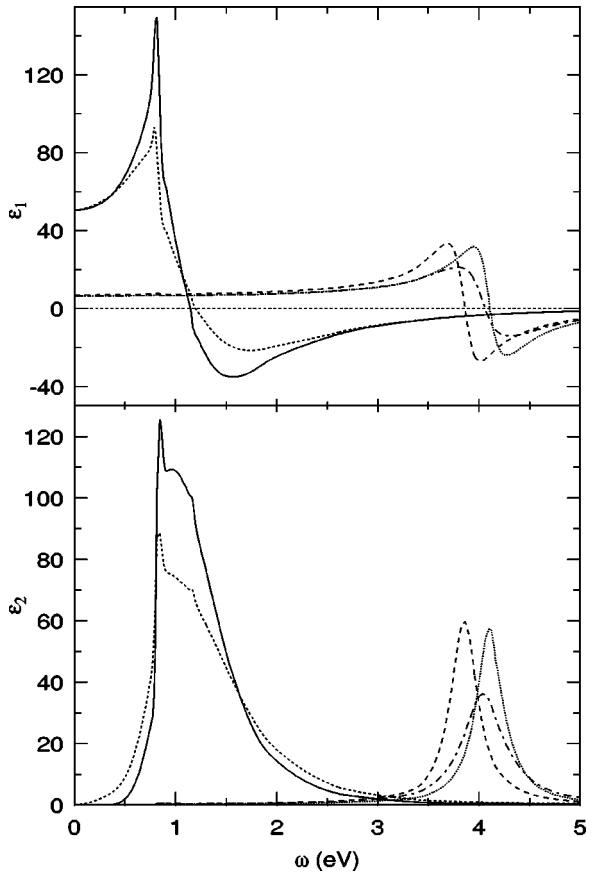

FIG. 3. The real and imaginary parts of the dielectric function of crystalline polyacetylene. Dashed curve: CNT; long-dashed curve: NCT; dot-dashed curve: QV; dotted curve: QV0; continuous curve: ALDA. The meanings of the abbreviations are explained in the text.

zation by its static limit is a good approximation in this case. This is not surprising because within the range of frequencies where the absorption has significant intensity and in the range of r_s values that are relevant for polyacetylene, which we checked to be $r_s \lesssim 2$, the coefficients $f_{xcL,T}(\rho_0,\omega)$ do not change much with respect to their values in the static limit. Like the QV0 spectrum, the NCT spectrum is obtained from values of $f_{xcL,T}(\rho_0,\omega)$ evaluated in their static limit. The only difference between the two approximations is the set of μ_{xc} values that is used. The NCT values are slightly lower than those of QV (in the relevant range of r_s values for polyacetylene). We observe that this difference leads to an NCT spectrum that lies a bit lower in energy than the QV0 spectrum. In fact, we see that the approximations for $f_{xcL,T}(\rho_0,\omega)$ that have nonzero values for μ_{xc} (NCT, QV, QV0), related to $f_{xcT}(\rho_0,0)$ by Eq. (46), lead to peaks in the absorption spectra that are shifted with respect to the ALDA spectrum. The influence of the frequency dependence of $f_{xcL,T}(\rho_0,\omega)$ for $\omega>0$ on the position and the shape of the peak is only small as we can see by comparing the CNT spectrum with the ALDA spectrum and the QV spectrum with the QV0 spectrum. These considerations imply a large dependence on the values of μ_{xc} and a relatively small dependence on the behavior of $f_{xcL,T}(\rho_0,\omega)$ for $\omega>0$ for the position and the shape of the spectrum in the 1D case. We note that the CNT behavior of $f_{xcL,T}(\rho_0,\omega)$ for $\omega>0$ does have influence on the intensity of the absorption as can be seen by comparing the CNT spectrum with the ALDA spectrum, but relative to the effect of μ_{xc} on the spectrum it seems to be small. Looking at the absorption spectrum in the 3D case we observe the same qualitative features as in the 1D spectrum. The difference between the QV and QV0 spectrum is somewhat larger, however, than in the 1D case. Still the contribution from μ_{xc} to the spectra seems to be the most important. Unfortunately, not much is known about the precise values of μ_{xc}. As mentioned above, NCT do not deem their values of μ_{xc} to be very accurate and it is not clear how accurate the values are of the Landau parameters calculated by Yasuhara and Ousaka[51] which were used by QV to obtain values for μ_{xc}. These calculations of the Landau parameters are the only recent calculations done for the three-dimensional electron gas.

We will now compare our results for the infinite polyacetylene chain with the results obtained by van Faassen *et al.* for polyacetylene oligomers. They showed that the static polarizability per unit chain length of these oligomers is largely reduced by including the VK functional in their calculations[18,19] with respect to the ALDA results, which substantially overestimate this quantity. Their results reproduce those of MP2 calculations. The absolute and relative reduction is increased with increasing chain length leading to

a reduction of about a factor of 3 for the longest oligomers that they calculated. Their VK results were obtained using the values for μ_{xc} from NCT. It is, however, difficult to obtain a quantitative comparison with their findings since this requires extrapolation of their results to infinite chain length, something that is not straightforward. From our NCT results in the real part in Fig. 2 we see the same effect as observed by van Faassen *et al.*, a large reduction of about a factor of 6 of our static polarizability per unit chain length with respect to the ALDA values. Our NCT result in the static limit should be an upper limit for the static polarizability per unit chain length of the polyacetylene oligomers of increasing chain length obtained by van Faassen *et al.* They furthermore showed that by including the VK functional in their calculations the oscillator strengths of low-lying excitations decrease and those of higher-lying excitations increase with respect to the oscillator strengths obtained in the ALDA when the length of the chain is increased.[20] We observe similar features in our absorption spectrum where the intensity of the absorption, which is proportional to the oscillator strength, in the NCT spectrum is reduced at low excitation energies and is increased at higher excitation energies with respect to the ALDA spectrum. However, when comparing the NCT spectra with results obtained from accurate calculations and experiment we see that the peak is shifted to too high energy. As mentioned in the Introduction, Rohlfing and Louie[30] performed BSE calculations on 1D polyacetylene and found the position of the peak in the absorption spectrum at 1.7 eV. Furthermore, the experimental results from measurements on 3D polyacetylene by Leising[33] also show the peak in the absorption spectrum at 1.7 eV. These results indicate that the peaks in the ALDA and CNT spectra appear at too low energy and the peaks in the NCT, QV, and QV0 spectra appear at too high energy. As was mentioned above, there seems to be a strong dependence of the shift of the peak position with respect to that in the ALDA spectrum on the parameter μ_{xc}. Actually, we can show that by steadily increasing the values for μ_{xc} from zero upwards (in the r_s-range relevant for polyacetylene) the peak smoothly "walks" away from the ALDA result to higher frequency. The two sets of values for μ_{xc} that are available, those calculated by NCT and QV, differ substantially for $r_s \gtrsim 2$. Because of the uncertainty in the theoretical values of μ_{xc} we choose to fit the position of the peak to the BSE result, which we find more reliable than the experimental result for reasons mentioned in the Introduction, for 1D polyacetylene with μ_{xc} as fitting parameter. We test this idea in a simple static scheme like the NCT and QV0 approximation. With this scheme and with μ_{xc} equal to 7.5×10^{-3} for $r_s \geqslant 1$, we can reproduce the position of the peak for 1D polyacetylene as found in the BSE spectrum. The behavior for small r_s was again taken to be quadratic. We note that there are probably other choices possible for μ_{xc} as a function of r_s that give the same result for the peak position. Using these values for μ_{xc} in the calculation of the absorption spectrum in the 3D case we find the peak at 1.8 eV compared to 1.7 eV in experiment. The results of these calculations of the absorption spectra can be found in Figs. 4 and 5. The real parts of the spectra are not reported but we note that the static values are not reduced to such a great extent with respect to the ALDA values as we found from the NCT, QV, and QV0 calculations. The static values are now reduced to 386 in the 1D case and 26.4 in the 3D case. The position of the peak in the absorption spectrum now being the same as the BSE result (1D) and almost the same as in experiment (3D), we can now compare the shape of the spectra. In the case of 1D polyacetylene, Rohlfing and Louie found a sharp peak in their absorption spectrum. This is clearly not reproduced in our spectrum as we find a very broad peak. In the case of 3D polyacetylene Puschnig and Ambrosch-Draxl[31] find by solving the BSE a peak with a full-width at half-maximum of 0.3 eV and a maximum of 180. Tiago *et al.*[32] find, also from BSE calculations, a peak at 1.7 eV with a full-width at half-maximum of 0.14 eV and a maximum of 350. Leising finds a peak at 1.7 eV with a full-width at half-maximum of 0.5 eV and a maximum of 30. We find a peak with a full-width at half-maximum of 0.7 eV and a maximum of 71. With respect

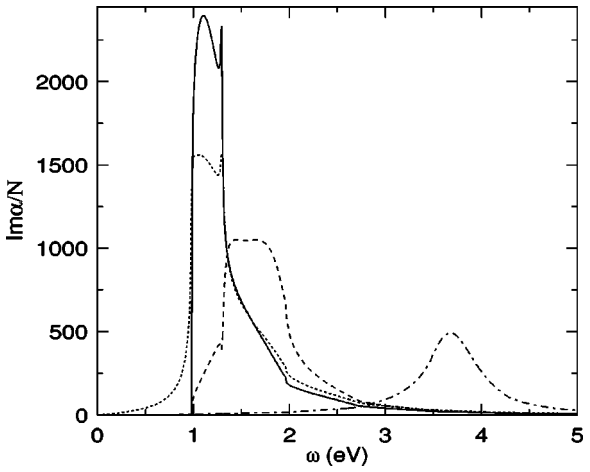

FIG. 4. The imaginary part of the polarizability per unit length of an infinite polyacetylene chain in a.u. Dashed curve: CNT; dot-dashed curve: QV; continuous curve: ALDA; long-dashed curve: fit. The meanings of the abbreviations are explained in the text.

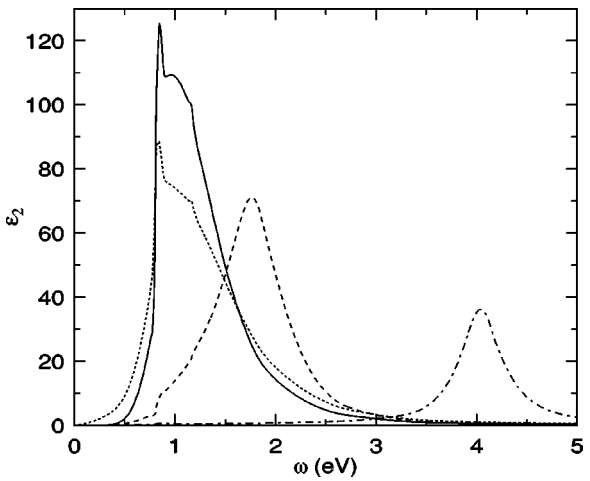

FIG. 5. The imaginary part of the dielectric function of crystalline polyacetylene. Dashed curve: CNT; dot-dashed curve: QV; continuous curve: ALDA; long-dashed curve: fit. The meanings of the abbreviations are explained in the text.

to the BSE results, the width of the peak in our absorption spectrum is too large and its height too small; the total intensity of the spectra are, however, comparable. In general we find that the peaks in the 1D and 3D absorption spectra are too broad. This can either be caused by a wrong choice of the μ_{xc} dependence on r_s, the wrong ω dependence of $f_{xcL,T}(\rho_0,\omega)$ (none in this case), or flaws in the VK functional itself. We note that including the ω dependence of $f_{xcL,T}(\rho_0,\omega)$ in the calculations through either the CNT or the QV parametrization will not solve this problem as it does not alter the width of the peaks, it mainly reduces their height (see Figs. 2 and 3).

VI. CONCLUSIONS

In this work we used the current density as the natural fundamental quantity in which to formulate TDDFT for extended systems. So-called time-dependent current density functional theory (TDCDFT) may provide an elegant way to account for contributions of nonlocal exchange-correlation effects. We introduced an efficient way to include the Vignale-Kohn current functional for the induced exchange-correlation vector potential into our self-consistent calculation scheme. In order to evaluate the Vignale-Kohn functional one has to have knowledge of the exchange-correlation kernels of the homogeneous electron gas $f_{xcL,T}(\rho_0,\omega)$ as a function of the density and as a function of the frequency. There exist two frequency-dependent parametrizations of $f_{xcL,T}(\rho_0,\omega)$, one by Conti, Nifosì, and Tosi (CNT) (Ref. 27) and the other by Qian and Vignale (QV).[28] We tested the effect of these parametrizations within the Vignale-Kohn functional on the calculation of linear response properties of polyacetylene, namely the polarizability per unit chain length of an infinite polyacetylene chain (1D) and the dielectric function of crystalline polyacetylene (3D). We showed that the two frequency-dependent parametrizations lead to very different results. Furthermore, we showed that the effect on the results caused by the frequency dependence of $f_{xcL,T}(\rho_0,\omega)$ is small with respect to the effect caused by the values of the transverse exchange-correlation kernel $f_{xcT}(\rho_0,\omega)$ in the limit $\omega\to 0$ by inspecting the two frequency-dependent parametrizations in their static limit. They correspond to the ALDA and QV0 for CNT and QV, respectively. It can be shown that the values for $f_{xcT}(\rho_0,\omega)$ in the limit $\omega\to 0$ are related to the exchange-correlation part of the shear modulus μ_{xc}.[44]

The results we obtain are in good qualitative agreement with the Vignale-Kohn results obtained for polyacetylene oligomers.[18–20] They are, however, very different from the results of calculations done on polyacetylene by solving the BSE. One of the main causes of this discrepancy is the lack of accurate values that are available for μ_{xc}. This is an important quantity as the positions of the peak in the absorption spectra depend strongly on it. When restoring this difference by fitting the peak position to BSE results with μ_{xc} as a parameter, we are able to obtain spectra that show the peaks at the right position but these peaks are too broad. This can be caused by our specific choice of μ_{xc} or by the wrong description of the frequency dependence of $f_{xcL,T}(\rho_0,\omega)$. It may even be a problem inherent to the Vignale-Kohn functional itself. But in order to be able to assess the merits of the Vignale-Kohn functional it is important to first obtain accurate values for μ_{xc} either by first-principle calculations or by some empirical fitting scheme.

APPENDIX: DERIVATION OF THE XC-VECTOR POTENTIAL

The exchange-correlation vector potential as written in Eq. (28) and in particular the $\partial_j(\tilde{\eta}_{xc}\partial_j u_i)$ term cannot easily be evaluated as such. Consider, therefore, the following vector identity:

$$[\boldsymbol{\nabla}\times[\tilde{\eta}_{xc}(\boldsymbol{\nabla}\times\mathbf{u})]]_i=\sum_j[\partial_j(\tilde{\eta}_{xc}\partial_i u_j)-\partial_j(\tilde{\eta}_{xc}\partial_j u_i)]. \tag{A1}$$

Let us work out the first term on the right-hand side a bit further,

$$\partial_j(\tilde{\eta}_{xc}\partial_i u_j)=\partial_i[\tilde{\eta}_{xc}\partial_j u_j+(\partial_j\tilde{\eta}_{xc})u_j]-(\partial_i\partial_j\tilde{\eta}_{xc})u_j-(\partial_i\tilde{\eta}_{xc})\times(\partial_j u_j), \tag{A2}$$

so that we can combine the two results, Eqs. (A1) and (A2), to arrive at the following expression for the traceless contribution to the viscoelastic stress tensor,

$$\sum_j\partial_j\sigma_{xc,ij}=\{-\boldsymbol{\nabla}\times[\tilde{\eta}_{xc}(\boldsymbol{\nabla}\times\mathbf{u})]\}_i+\sum_j\left(2\partial_j(\tilde{\eta}_{xc}\partial_i u_j)-\frac{2}{3}\partial_i(\tilde{\eta}_{xc}\partial_j u_j)+\partial_i(\tilde{\zeta}_{xc}\partial_j u_j)\right) \tag{A3}$$

$$=\{-\boldsymbol{\nabla}\times[\tilde{\eta}_{xc}(\boldsymbol{\nabla}\times\mathbf{u})]\}_i+\partial_i\left[\left(\frac{4}{3}\tilde{\eta}_{xc}+\tilde{\zeta}_{xc}\right)\partial_j u_j+2(\partial_j\tilde{\eta}_{xc})u_j\right]-2\sum_j[\partial_i\partial_j\tilde{\eta}_{xc}u_j+(\partial_i\tilde{\eta}_{xc})\partial_j u_j]. \tag{A4}$$

Using the nabla operator, we arrive at the following result for the exchange-correlation vector potential field,

$$-\frac{1}{\rho_0}\boldsymbol{\nabla}\cdot\sigma_{xc}=-\boldsymbol{\nabla}\left[\frac{1}{\rho_0}\left(\frac{4}{3}\tilde{\eta}_{xc}+\tilde{\zeta}_{xc}\right)(\boldsymbol{\nabla}\cdot\mathbf{u})+2\frac{1}{\rho_0}\boldsymbol{\nabla}\tilde{\eta}_{xc}\cdot\mathbf{u}\right]+\boldsymbol{\nabla}\times\left(\frac{1}{\rho_0}\tilde{\eta}_{xc}(\boldsymbol{\nabla}\times\mathbf{u})\right)-\frac{\boldsymbol{\nabla}\rho_0}{\rho_0^2}\left[\left(\frac{4}{3}\tilde{\eta}_{xc}+\tilde{\zeta}_{xc}\right)\times(\boldsymbol{\nabla}\cdot\mathbf{u})+2\boldsymbol{\nabla}\tilde{\eta}_{xc}\cdot\mathbf{u}\right]+\tilde{\eta}_{xc}\frac{\boldsymbol{\nabla}\rho_0}{\rho_0^2}\times(\boldsymbol{\nabla}\times\mathbf{u})+\frac{2}{\rho_0}[\boldsymbol{\nabla}\boldsymbol{\nabla}\tilde{\eta}_{xc}\cdot\mathbf{u}+\boldsymbol{\nabla}\tilde{\eta}_{xc}(\boldsymbol{\nabla}\cdot\mathbf{u})]. \tag{A5}$$

We obtain

$$-\frac{1}{\rho_0}\boldsymbol{\nabla}\cdot\sigma_{xc}\doteq\frac{i\omega}{c}\delta\mathbf{A}_{xc}=\boldsymbol{\nabla}\delta u_{xc}+\frac{i\omega}{c}\delta\mathbf{a}_{xc}+\frac{i\omega}{c}\boldsymbol{\nabla}\times\delta\mathbf{b}_{xc}, \tag{A6}$$

where δu_{xc}. $\delta\mathbf{a}_{xc}$, and $\delta\mathbf{b}_{xc}$ are given in Eqs. (51)–(53).

[1] E. Runge and E. K. U. Gross, Phys. Rev. Lett. **52**, 997 (1984).
[2] E. K. U. Gross and W. Kohn, Adv. Quantum Chem. **21**, 255 (1990).
[3] E. K. U. Gross, J. F. Dobson, and M. Petersilka, Top. Curr. Chem. **181**, 81 (1996).
[4] R. van Leeuwen, Int. J. Mod. Phys. B **15**, 997 (2001).
[5] A. K. Dhara and S. K. Ghosh, Phys. Rev. A **35**, 442 (1987).
[6] S. K. Ghosh and A. K. Dhara, Phys. Rev. A **38**, 1149 (1988).
[7] G. D. Mahan and K. R. Subbaswami, *Local Density Theory of Polarizability* (Plenum Press, New York, 1990).
[8] G. Onida, L. Reining, and A. Rubio, Rev. Mod. Phys. **74**, 601 (2002).
[9] O.-J. Wacker, R. Kümmel, and E. K. U. Gross, Phys. Rev. Lett. **73**, 2915 (1994).
[10] G. Vignale and W. Kohn, Phys. Rev. Lett. **77**, 2037 (1996).
[11] G. Vignale and W. Kohn, in *Electronic Density Functional Theory: Recent Progress and New Directions*, edited by J. Dobson, M. P. Das, and G. Vignale (Plenum Press, New York, 1998).
[12] X. Gonze, P. Ghosez, and R. W. Godby, Phys. Rev. Lett. **74**, 4035 (1995); **78**, 294 (1997).
[13] P. Nozières and D. Pines, *The Theory of Quantum Liquids* (Perseus Books, Cambridge, MA, 1999), Chap. 4.
[14] Y.-H. Kim and A. Görling, Phys. Rev. B **66**, 035114 (2002); Phys. Rev. Lett. **89**, 096402 (2002).
[15] R. van Leeuwen, in *Progress in Nonequilibrium Green's Functions II*, edited by M. Bonitz and D. Semkat (World Scientific, Singapore, 2003), p. 427.
[16] F. Sottile, V. Olevano, and L. Reining, Phys. Rev. Lett. **91**, 056402 (2003).
[17] G. Adragna, R. del Sole, and A. Marini, Phys. Rev. B **68**, 165108 (2003).
[18] M. van Faassen, P. L. de Boeij, R. van Leeuwen, J. A. Berger, and J. G. Snijders, Phys. Rev. Lett. **88**, 186401 (2002).
[19] M. van Faassen, P. L. de Boeij, R. van Leeuwen, J. A. Berger, and J. G. Snijders, J. Chem. Phys. **118**, 1044 (2003).
[20] M. van Faassen and P. L. de Boeij, J. Chem. Phys. **121**, 10707 (2004).
[21] S. J. A. van Gisbergen, P. R. T. Schipper, O. V. Gritsenko, E. J. Baerends, J. G. Snijders, B. Champagne, and B. Kirtman, Phys. Rev. Lett. **83**, 694 (1999).
[22] P. L. de Boeij, F. Kootstra, J. A. Berger, R. van Leeuwen, and J. G. Snijders, J. Chem. Phys. **115**, 1995 (2001).
[23] D. M. Ceperley and B. J. Alder, Phys. Rev. Lett. **45**, 566 (1980).
[24] S. H. Vosko, L. Wilk, and M. Nusair, Can. J. Phys. **58**, 1200 (1980).
[25] E. K. U. Gross and W. Kohn, Phys. Rev. Lett. **55**, 2850 (1985); **57**, 923 (1986).
[26] N. Iwamoto and E. K. U. Gross, Phys. Rev. B **35**, 3003 (1987).
[27] S. Conti, R. Nifosì, and M. P. Tosi, J. Phys.: Condens. Matter **9**, L475 (1997).
[28] Z. Qian and G. Vignale, Phys. Rev. B **65**, 235121 (2002).
[29] P. Vogl and D. K. Campbell, Phys. Rev. B **41**, 12 797 (1990).
[30] M. Rohlfing and S. G. Louie, Phys. Rev. Lett. **82**, 1959 (1999).
[31] P. Puschnig and C. Ambrosch-Draxl, Phys. Rev. Lett. **89**, 056405 (2002); Synth. Met. **135–136**, 415 (2003).
[32] M. L. Tiago, M. Rohlfing, and S. G. Louie, Phys. Rev. B **70**, 193204 (2004).
[33] G. Leising, Phys. Rev. B **38**, 10 313 (1988).
[34] J.-W. van der Horst, P. A. Bobbert, and M. A. J. Michels, Phys. Rev. B **66**, 035206 (2002).
[35] P. Hohenberg and W. Kohn, Phys. Rev. **136**, B864 (1964).
[36] F. Kootstra, P. L. de Boeij, and J. G. Snijders, J. Chem. Phys. **112**, 6517 (2000).
[37] F. Kootstra, P. L. de Boeij, and J. G. Snijders, Phys. Rev. B **62**, 7071 (2000).
[38] G. Breit, Phys. Rev. **34**, 553 (1929); **39**, 616 (1932).
[39] O. L. Brill and B. Goodman, Am. J. Phys. **35**, 832 (1967).
[40] C. A. Ullrich and G. Vignale, Phys. Rev. Lett. **87**, 037402 (2001).
[41] C. A. Ullrich and G. Vignale, Phys. Rev. B **65**, 245102 (2002).
[42] G. Vignale, C. A. Ullrich, and S. Conti, Phys. Rev. Lett. **79**, 4878 (1997).
[43] C. A. Ullrich and K. Burke, J. Chem. Phys. **121**, 28 (2004).
[44] S. Conti and G. Vignale, Phys. Rev. B **60**, 7966 (1999).
[45] H. M. Böhm, S. Conti, and M. P. Tosi, J. Phys.: Condens. Matter **8**, 781 (1996).
[46] R. Nifosì, S. Conti, and M. P. Tosi, Phys. Rev. B **58**, 12 758 (1998).
[47] J. Lindhard, Mat. Fys. Medd. K. Dan. Vidensk. Selsk. **28**(8), 1 (1954).
[48] A. J. Glick and W. F. Long, Phys. Rev. B **4**, 3455 (1971).
[49] A. Holas and K. S. Singwi, Phys. Rev. B **40**, 158 (1989).
[50] S. Ichimaru, Rev. Mod. Phys. **54**, 1017 (1982).
[51] H. Yasuhara and Y. Ousaka, Int. J. Mod. Phys. B **6**, 3089 (1992).
[52] G. te Velde and E. J. Baerends, Phys. Rev. B **44**, 7888 (1991); J. Comput. Phys. **99**, 84 (1992).
[53] C. Fonseca Guerra, O. Visser, J. G. Snijders, G. te Velde, and E. J. Baerends, in *Methods and Techniques in Computational Chemistry*, edited by E. Clementi and G. Corongiu (STEF, Cagliary, 1995), p. 305.
[54] G. te Velde, F. M. Bickelhaupt, E. J. Baerends, C. Fonseca Guerra, S. J. A. van Gisbergen, J. G. Snijders, and T. Ziegler, J. Comput. Chem. **22**, 931 (2001).
[55] F. Herman and S. Skillman, *Atomic Structure Calculations* (Prentice-Hall, Englewood Cliffs, NJ, 1963).
[56] G. Lehmann and M. Taut, Phys. Status Solidi B **54**, 469 (1972).